

THE NATURE OF A MOVING DISLOCATION BAND  
FOUND WHEN ZINC IS DIFFUSED INTO GALLIUM ARSENIDE

GPO PRICE \$ \_\_\_\_\_

CFSTI PRICE(S) \$ \_\_\_\_\_

Hard copy (HC) 2.00

Microfiche (MF) 1.50

H. B. Kim

R. L. Longini

# 653 July 65

Prepared under Contract No. NAS 8-5269 by  
Electrical Engineering Department  
Carnegie Institute of Technology  
Pittsburgh, Pennsylvania 15213  
for  
National Aeronautics and Space Administration

FACILITY FORM 502

**N66 32431**

(ACCESSION NUMBER)

37

(PAGES)

CR-76755

(NASA CR OR TMX OR AD NUMBER)

(THRU)

1

(CODE)

26

(CATEGORY)

## 1. INTRODUCTION

A moving band of dislocations and a non-planar p-n junction are observed to be produced by diffusion of zinc into gallium arsenide. The leading edge of the band is considered to be the result of the steep front of the diffusion profile. Here it is theorized that zinc diffuses interstitially with zinc mostly falling into substitutional positions and becoming relatively immobile substitutional atoms at a band of dislocations which is induced by the concentration gradient stress. It has been shown by Chang and Pearson<sup>(1)</sup> that zinc diffuses in gallium arsenide by an interstitial-substitutional mechanism first proposed by Longini<sup>(2)</sup>, and that the diffusion process is dominated by the highly mobile interstitials even though they are outnumbered by orders of magnitude by the relatively immobile substitutionals.

The largest gradient develops at the leading edge of the dislocation band, and results in stresses exceeding the elastic limit. To relieve the stress, edge dislocations (or partials) are introduced at the leading edge of the band. Schwuttke and Rupprecht<sup>(3)</sup> reported from x-ray diffraction measurements that diffusion of large concentrations of zinc induces defects of bent stacking faults of the Lomer-Cottrell type with the stair-rod dislocations parallel to the (111) diffusion planes when zinc is diffused at 850° into Te-doped substrate. The dislocation band, being at the steep front of the diffusion profile, provides the region of high transition probability bordering two contrasting high and low concentration regions. As the high transition rate at the dislocations of the leading edge of the band rapidly builds up the concentration of the substitutional zinc, the large gradient is moved forward into the material and results in stresses that induce edge dislocations, thus propagating the band further into the host crystal. A residual flux of interstitials beyond those that "condense" at dislocations, continues to diffuse beyond the band, and eventually finds sites for transition to become substitutional atoms. A non-planar

p-n junction forms beyond the band. Its lack of planarity is due to the non-uniform distribution of sites for these transitions to substitutional positions. Some experimental observations on the moving dislocation band and the p-n junction planarity under various diffusion conditions have been explained qualitatively in terms of the moving band model.

## II. EXPERIMENTAL PROCEDURES

Single crystal n-type Te-doped GaAs wafers having (111) faces orientation are prepared to have either lapped or polished (chemically or mechanically) surface. Five micron  $\text{Al}_2\text{O}_3$  grit was used for the final step of the lapped surface. The mechanically polished surface was prepared by polishing on a rotating pellen cloth using first the premixed solution of Linde A :  $\text{H}_2\text{O}$  :  $\text{H}_2\text{O}_2$  :: 10 : 4 : 1 and then the solution of Linde B :  $\text{H}_2\text{O}$  :  $\text{H}_2\text{O}_2$  :: 10 : 5 : 1 by volume. The chemically polished surface was prepared by etching in 4-6 per cent sodium hypochloride at  $75^\circ\text{C}$  for 2-5 minutes for {111} A surface, and, for {111} B surface, by etching in  $\text{H}_2\text{SO}_4$  :  $\text{H}_2\text{O}$  :  $\text{H}_2\text{O}_2$  :: 8 : 1 : 1 while the wafer was fastened to a flat quartz plate and spinning on another plate within a rotating beaker.

The prepared samples were loaded into a clean quartz ampule (about  $20\text{ cm}^3$  in volume) together with the diffusant and the excess arsenic designed to produce various pressures in the range of 0-5 atm. The ampules were evacuated to about  $10^{-6}$  torr and sealed off. The sealed ampule was placed in the furnace at the region of the flat temperature profile as shown in Fig. 1. At the end of the diffusion the ampule was quenched in water, such that condensation was localized at one end of the ampule away from the sample.

On the {111} A surface the samples were etched with the Schell etch<sup>(4)</sup> ( $\text{HNO}_3$  :  $\text{H}_2\text{O}$  :: 1:2), and the etch pit density was determined every 3-8 microns through the diffused region and beyond the p-n junction into the undoped substrate, and obtained the etch pit density profile.

\* 30 per cent strength  $\text{H}_2\text{O}_2$

\*\* 98 per cent strength  $\text{H}_2\text{SO}_4$

φ 70 per cent strength  $\text{HNO}_3$

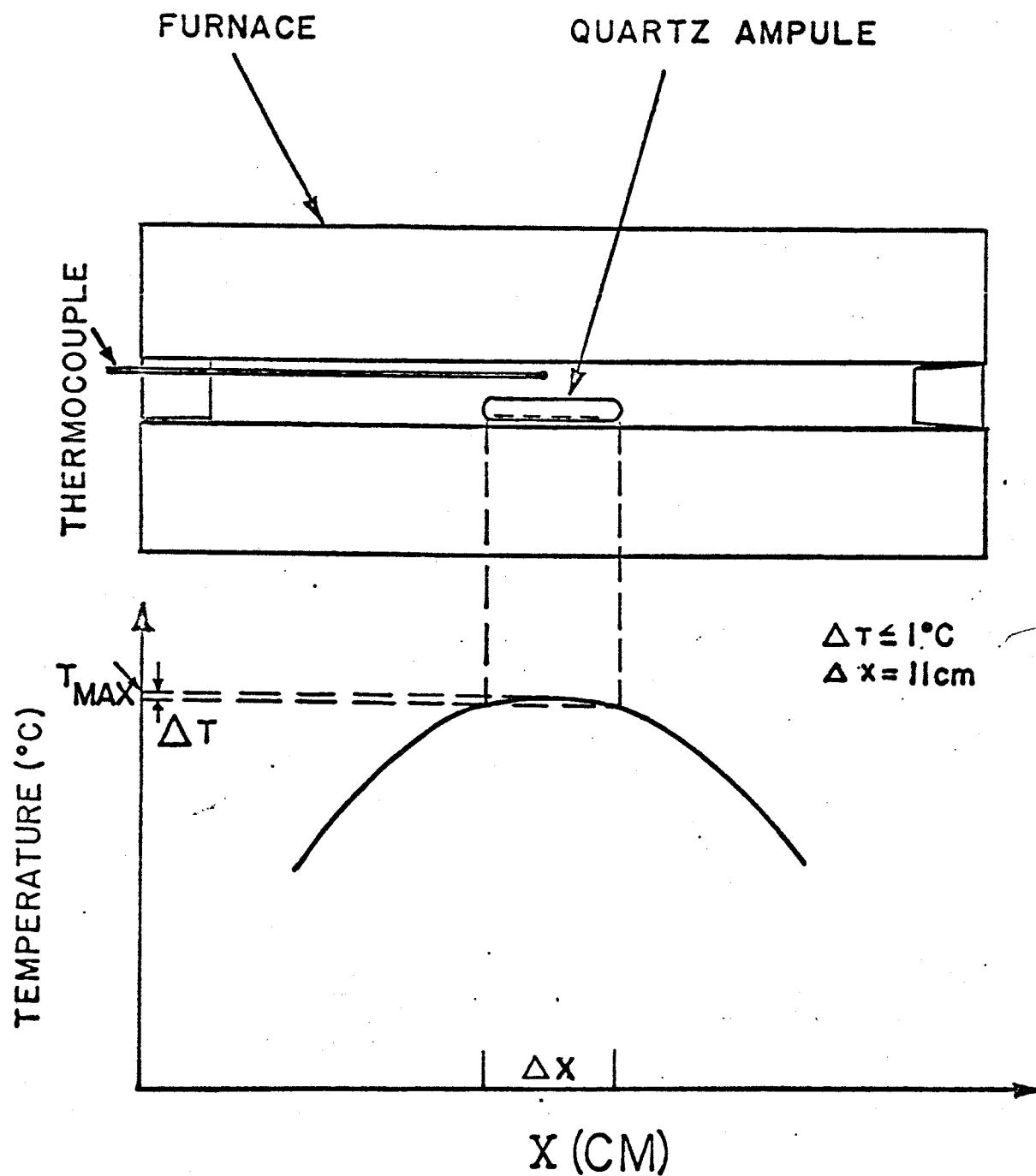


Figure 1. Diffusion furnace and its temperature profile measured with the furnace empty.

The line, P, and the etch pit band, Q, were rendered visible after etching the cleaved  $\{110\}$  surface for 50-90 seconds in the Schell etch at the room temperature.

The presence of the solute zinc atoms (Pauling's tetrahedral radius of  $1.31\text{\AA}$ ) in the host gallium atom sites (tetrahedral radius of  $1.26\text{\AA}$ ) in such a large concentration as of  $10^{20}\text{ cm}^{-3}$  results in an increase in the lattice constant. When such a doped region of the crystal is contiguous with an undoped region, stresses are produced due to the lattice mismatch, hence dislocations will be generated in the transition region to relieve the stress. The energy available is thus compensated only by the edge component of dislocations. Therefore we may expect more pure edge dislocations than the  $60^\circ$  - dislocations that are expected due to ordinary stressing, and we may expect practically no  $30^\circ$  - dislocations. The characteristics of the Schell etch pits on the  $111\text{ A}$  surface of GaAs as shown in Fig. 2, were investigated by Abrahams and Ekstrom<sup>(5)</sup>. They have established quantitative agreement between the etch pit density and Nye's theory on plastic deformation and have concluded that every edge dislocation results in a Schell etch pit. Thus we assume that these etch pits as shown in Fig. 2 may be ascribed to be the individual dislocations of the network with predominant edge type components.

### III. RESULTS

The line, P, and the etch pit band, Q, observed on a cleaved  $\{110\}$  surface as shown in Fig. 3 were examined with respect to the etch pit density profile and the electrical characteristics. The peak of the etch pit density profile of  $\{11\bar{1}\}\text{A}$  surfaces coincides with the etch pit band, Q, observed on cleaved  $\{110\}$  surface. The etch pit density drops rapidly for  $x > d_Q$  and produces the sharp leading edge of the etch pit band. The degree of the sharpness of the leading edge can be seen by the gradient of the etch pit density profile for  $x > d_Q$  and also the thickness of the etch pit band, Q, as shown from the

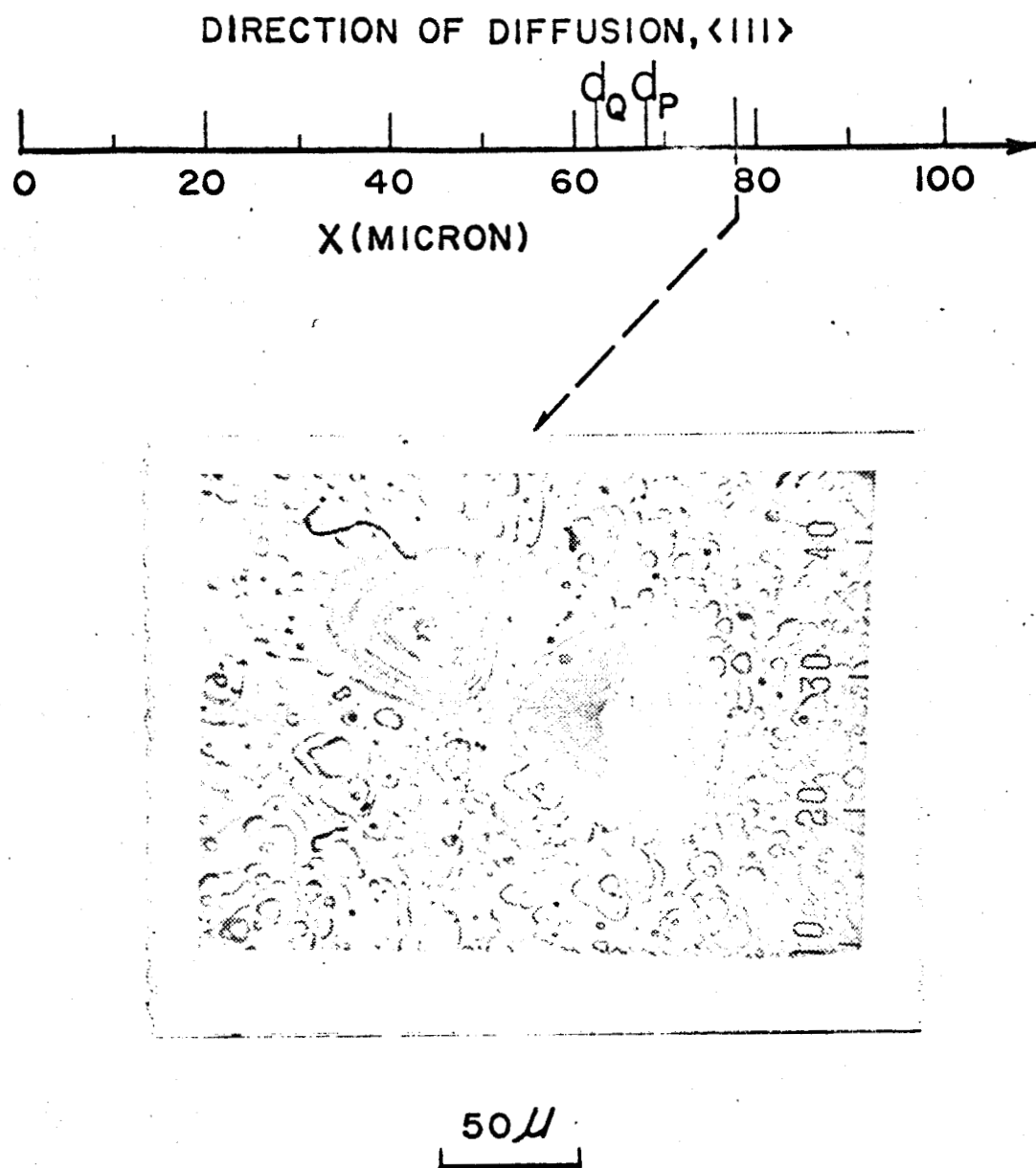
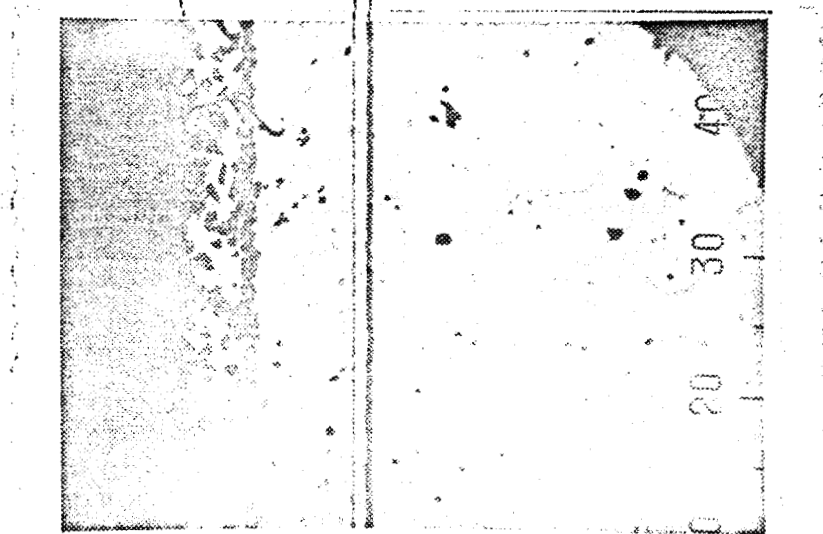
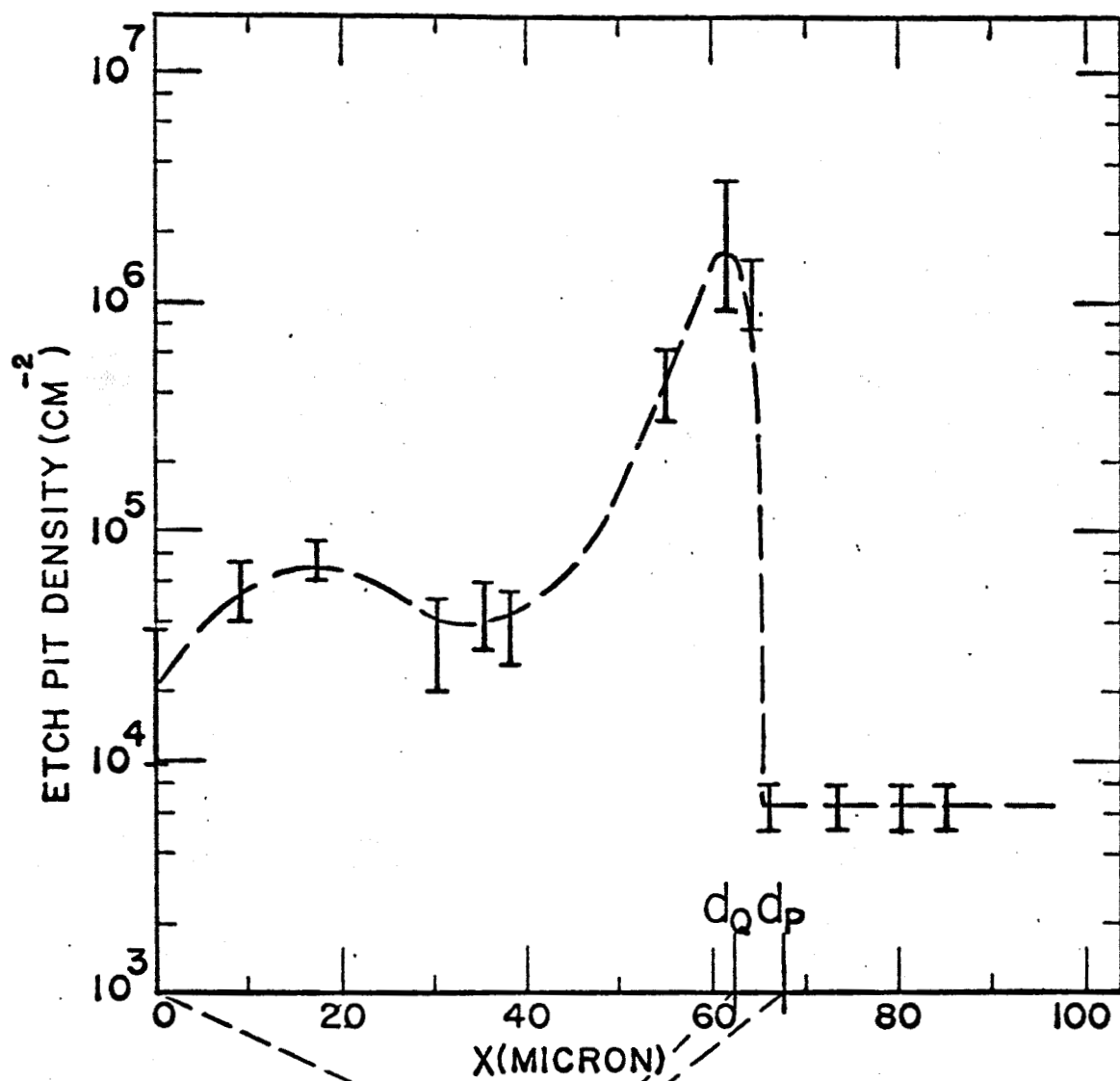


Figure 2. Schell etch pits observed on a  $\langle 111 \rangle$  surface and its location, which is in the "virgin" region.



L-32  
200x

Figure 3. The etch pit density profile and the photomicrograph of the etch pit band, Q, and the line, P, and their correlations to the peak of the etch pit density profile. L-32 diffusion condition:  $As_4 O = 1.12 \text{ atm.}$ , and chemically polished surface.

comparison of Figures 3 and 4. At  $x = d_p$  the etch pit density is equal to that of the "virgin" region. We have observed from the etch pit density profile that the etch pit band, Q, corresponds to the peak of the etch pit density profile and hence to the leading edge of the dislocation band, and that the magnitude,  $d_Q$  corresponds to the position of the deepest portion of the dislocation band.

Two examinations of the observed etch pit band, Q, and the line, P, are made individually with respect to their electrical characteristics. 1). Hot probe technique was used to determine the p- and n-type surfaces after every 3 to 8 microns of material were removed through the diffused region and beyond the p-n junction to the undoped substrate. The results of such measurements indicate that the line, P, corresponds to a p-n junction. 2). A more reliable technique of identifying a p-n junction without destroying the sample is the scanning electron microscope technique<sup>6</sup> developed by the Westinghouse Research Laboratories. The principle micrographs used in this work were obtained by the secondary electron video signal, by the "cathodo-voltage" generated by the scanning electron beam, and by mixing the two. Fig. 5B shows the micrograph of SEVS on a surface with and without externally applied bias. Figure 6C shows the two micrographs being superimposed into one: one of the "C-V" only, which was scanned only in the lower half, and the other of the SEVS. The results all conclude that the line, P, is a p-n junction.

It is observed that the magnitudes,  $d_Q$  and  $d_p$ , and the sharpness of the dislocation band are dependent upon the diffusion conditions such as the diffusion temperature, the excess arsenic, and the surface conditions. Both  $d_Q$  and  $d_p$  increase with increasing diffusion temperature and decrease with increasing excess arsenic as shown in Figures 7 and 8.  $d_p$  increases with increasing roughness of the surface condition, but  $d_Q$  remains reasonably constant as shown in Figures 9B and 10B. The degree of the sharpness of the dislocation band is increased with increasing excess arsenic, and is decreased with increasing diffusion temperature and with increasing roughness of the surface condition, e.g. Figures 9B and 10B. The distribution of the etch pits on III



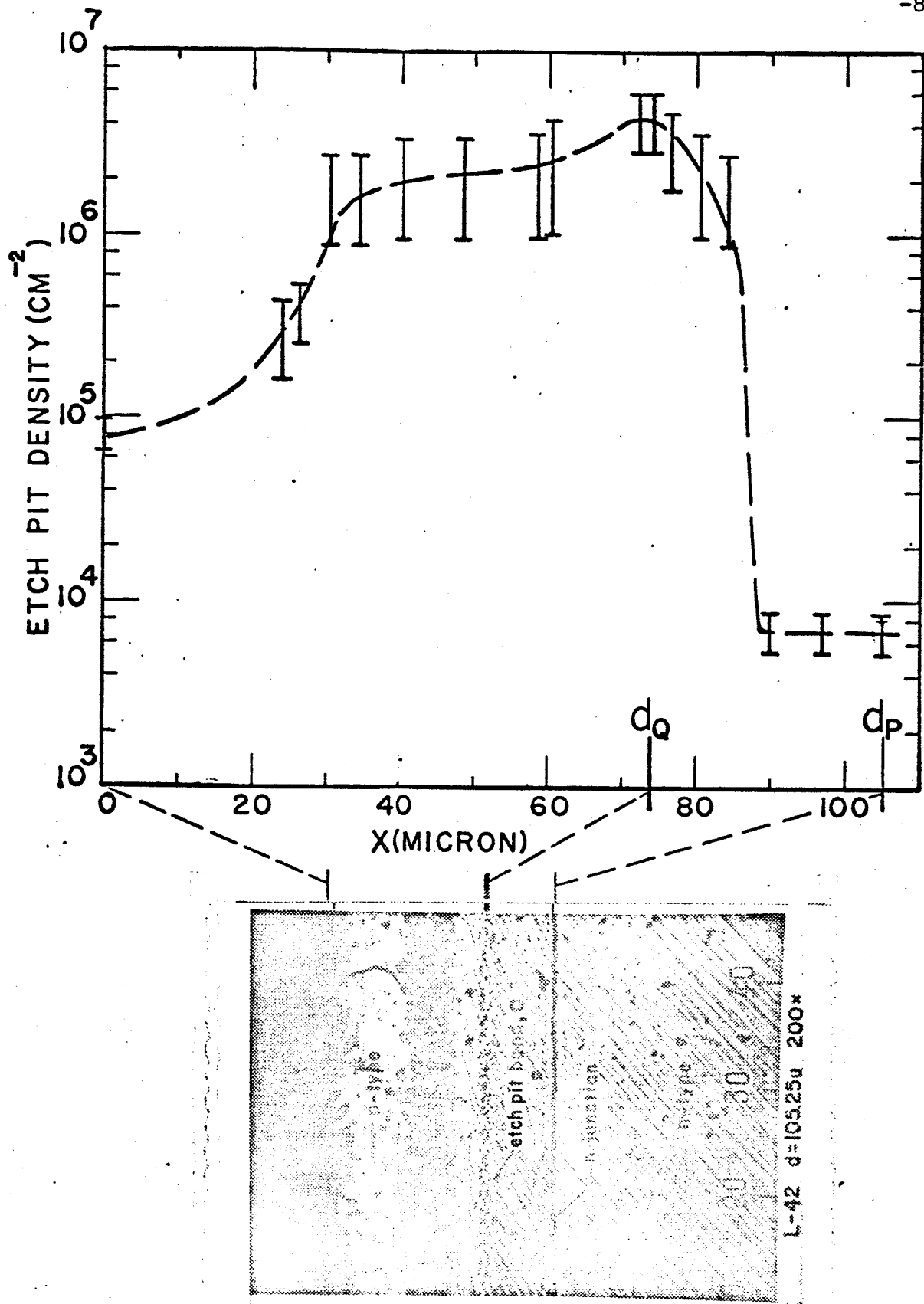


Figure 4. The etch pit density profile and the photomicrograph of the etch pit band, Q, and the line, P, and their correlations to the peak of the etch pit density profile. L-42 diffusion condition:  $As_4 O = .055$  atm., and lapped surface.

-9

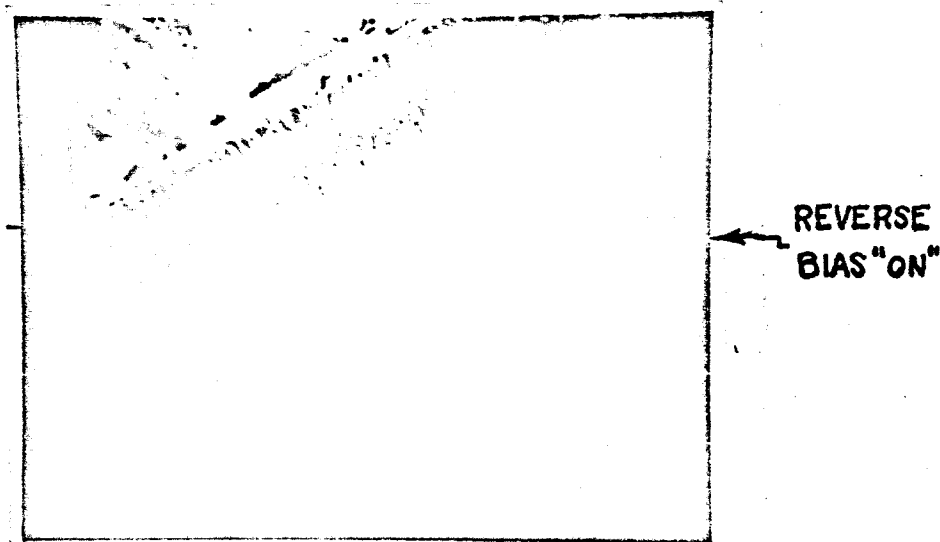


Figure 5. A scanning electron micrograph of the cleaved 110 surface of the diode video signal only without the externally applied bias, by SEVS only with the reverse bias of 4 volts being applied in the middle of the scanning.



Figure 6. Scanning electron micrographs of the "cathode-voltage" observations on the cleaved 110 surface of the diode. The "C-V" only, which was scanned only in the lower portion, and the other of the SEVS without the externally applied bias are superimposed.

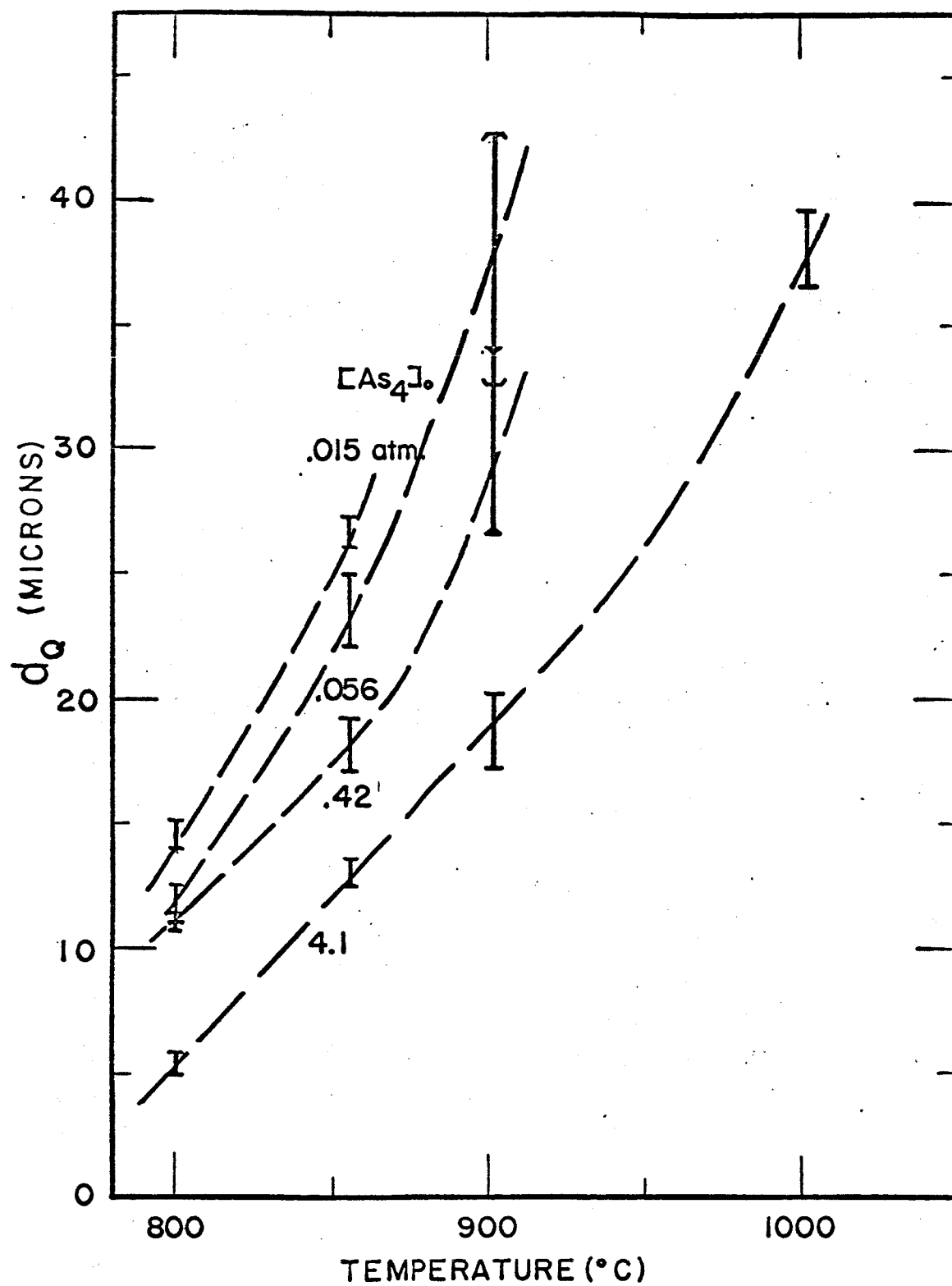


Figure 7. The depth of the etch pit band,  $d_0$ , against the diffusion temperature at various excess arsenic pressures.  $t_d = 3$  hrs.

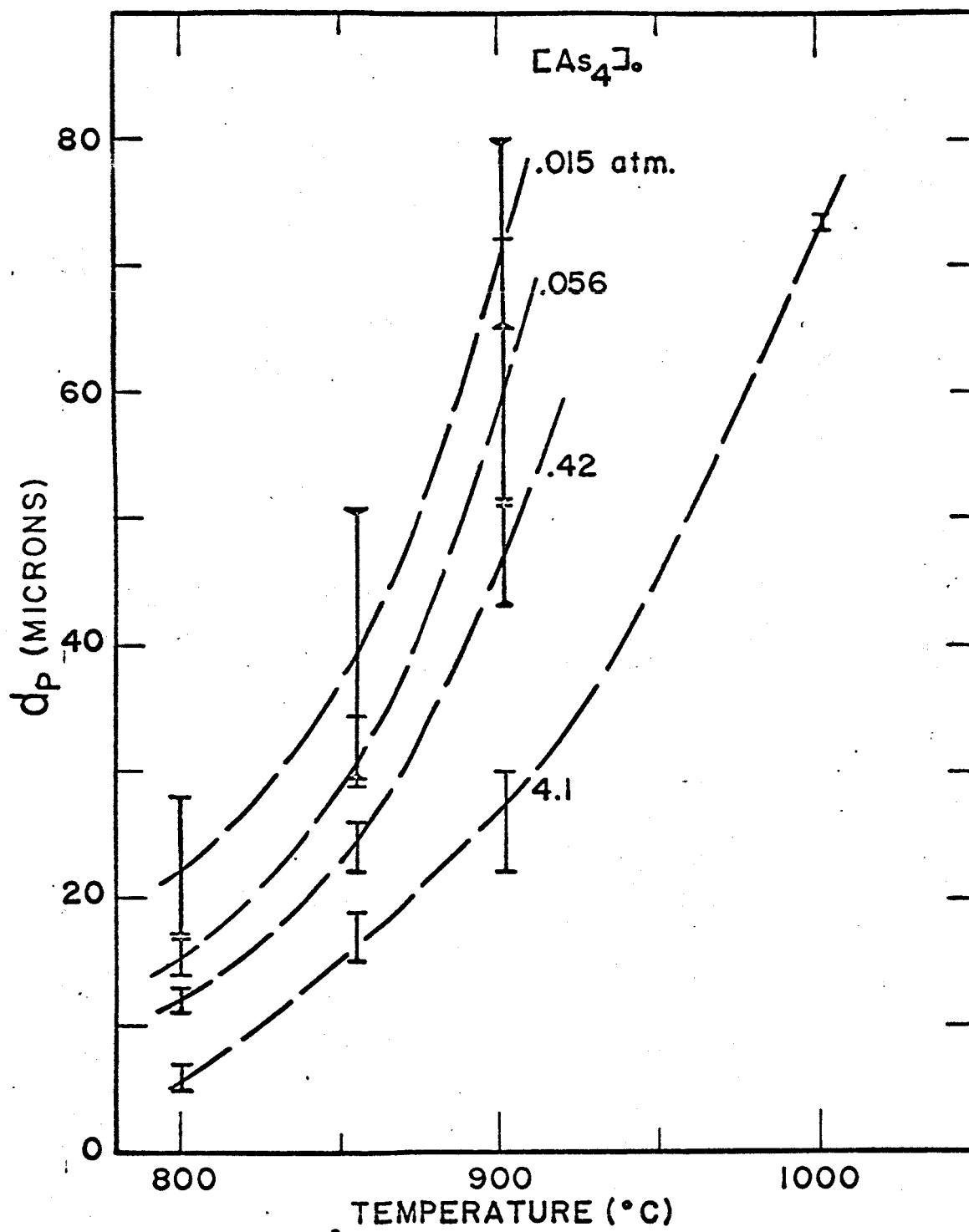


Figure 8. The depth of the p-n junction,  $d_p$ , against the diffusion temperature at various excess arsenic pressures.  $t_d = 3$  hrs.

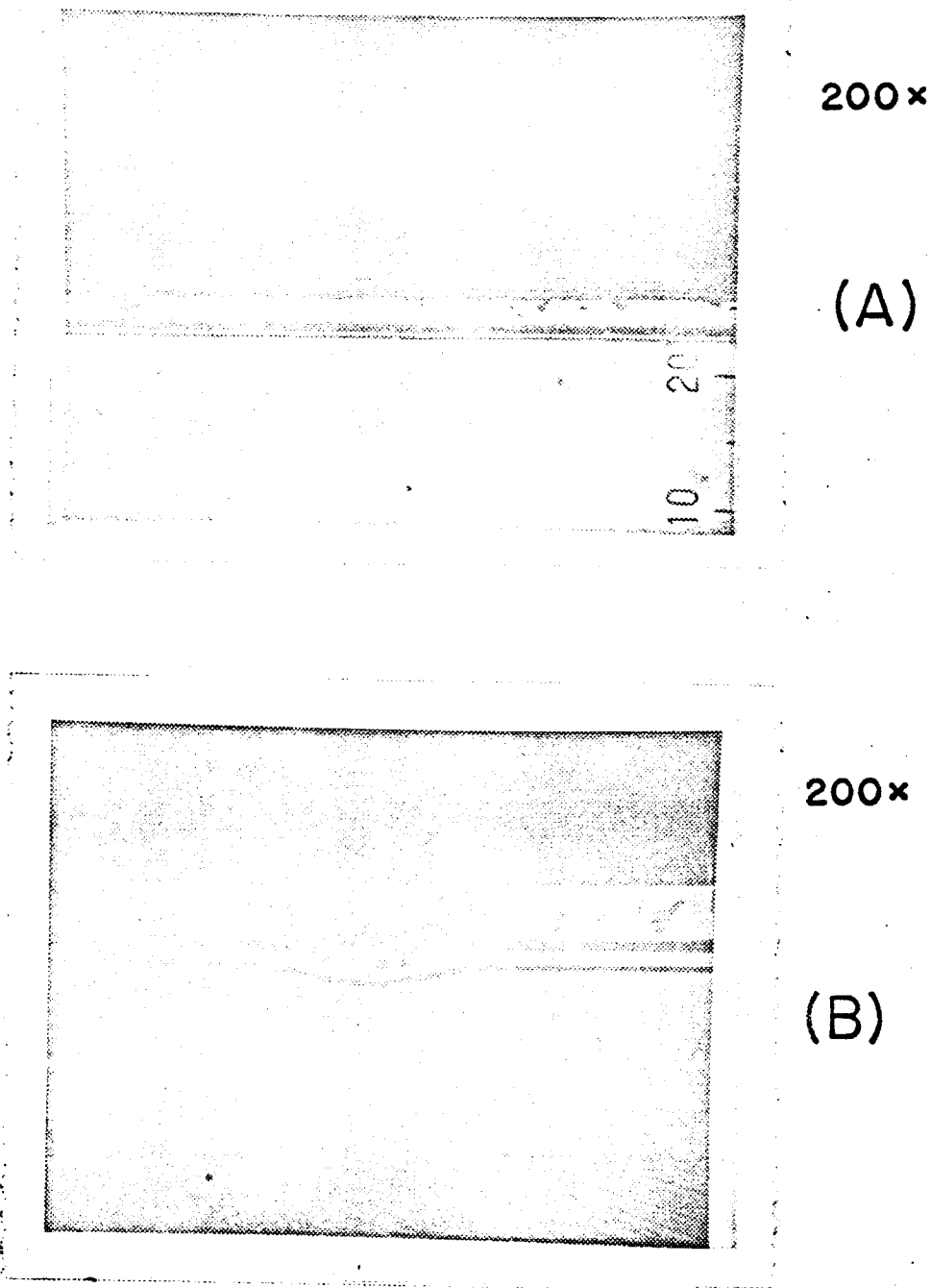


Figure 9. Photomicrographs of the observations on the sharpness of Q, on the distribution of the "defect-X", and the planarity of P.

(A) L-71 diffusion conditions:  $T = 855^{\circ}\text{C}$ ,  $\text{As}_{40} = 4.1 \text{ atm.}$  and chemically polished surface.

(B) L-72 diffusion conditions:  $T = 855^{\circ}\text{C}$ ,  $\text{As}_{40} = .015 \text{ atm.}$ , and chemically polished surface.

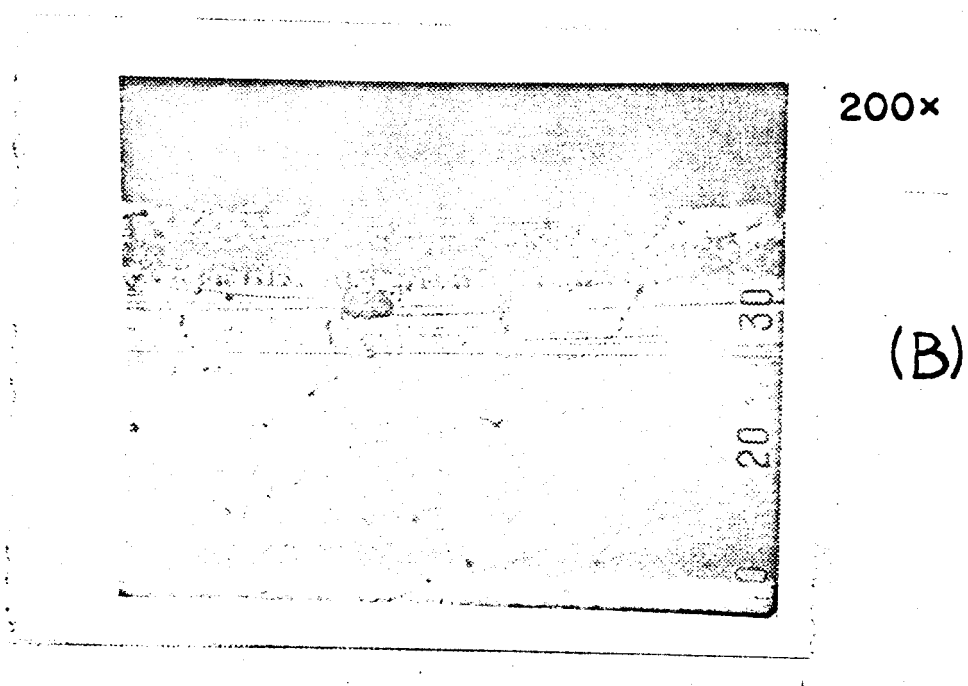
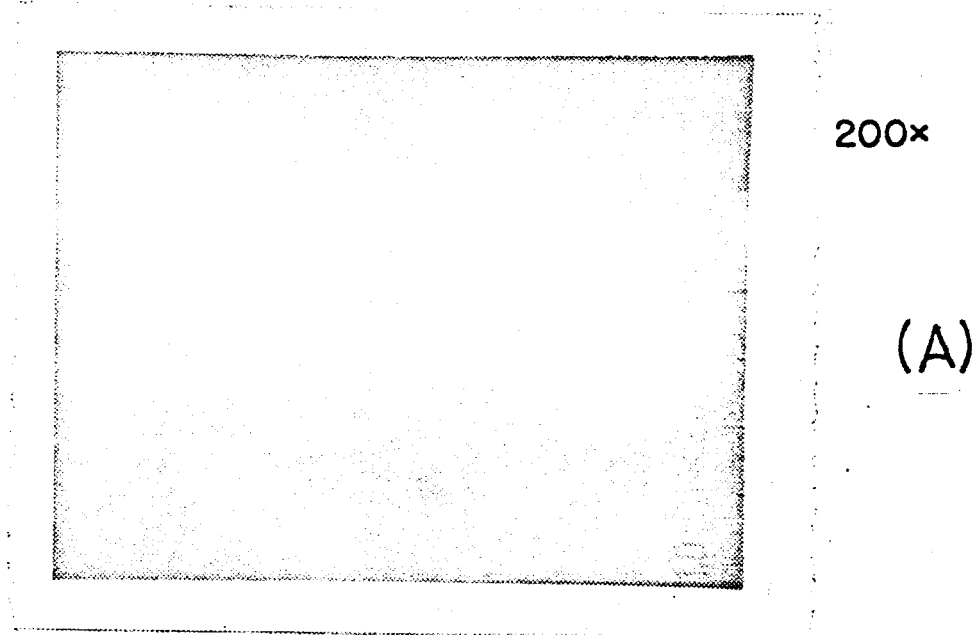


Figure 10. (a) L-68 diffusion conditions:  $T = 855^{\circ}\text{C}$ ,  $\text{As}_4\text{O} = .056 \text{ atm.}$ , and chemically polished surface. (b) L-72 diffusion conditions:  $T = 855^{\circ}\text{C}$ ,  $\text{As}_4\text{O} = .015 \text{ atm.}$ , and lapped surface.

surfaces was uniform for the lapped surface, whereas it was non-uniform for the polished surface as shown in Fig. 11A, B, and C.

#### IV. THEORETICAL CONSIDERATION

As previously stated, it is theorized here that zinc diffuses interstitially with the zinc mostly becoming substitutional and relatively immobile at the band of dislocation. The restricted volume of the dislocation band permits regions to exist where the interstitial zinc is far from its equilibrium relationship with substitutional zinc. It is, rather, the result of rapid diffusion from regions of higher concentration. The diffusion profile may thus be divided into three regions as shown in Fig. 12. Region I corresponds to the region with high concentration of its immobile substitutional zinc left behind the leading edge of the dislocation band. Region II corresponds to the region of the leading edge of the dislocation band. Region III corresponds to the region beyond the leading edge of the band. In Fig. 12A a theoretical zinc substitutional concentration profile of the moving band model is shown for the three regions. This can be compared to the diffusion profile obtained by Chang and Pearson<sup>(1)</sup> as shown in Fig. 13. The similarity of the diffusion profile to the model is observed up to and including Region II, but the experimental diffusion profile corresponding to Region III was not given. The isoconcentration (June, 1964) technique has no region where there is a net transition rate from one form to another and so these curves show no region of abrupt change of tracer zinc concentration. The thickness,  $\delta$ , of Region II is very small, and the substitutional species is rather spread out so that this characteristic is not obvious from the diffusion profile of Chang and Pearson. However, in view of the experimental observations of the dislocation band in our experiments, there must be a region of high transition probability. We assume that the substitutional zinc concentration at the dislocation band remains constant



L-32

200x

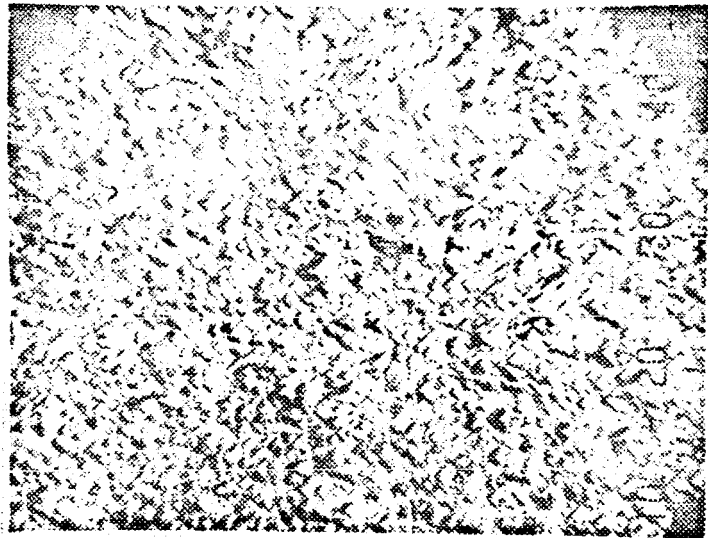
(A)



L-46

200x

(B)



L-42

200x

(C)

Figure 11. Photomicrographs of the etch pit density on the 111 surfaces.  
 (A) at  $X = 55.1u$ ;  $d_0 = 62.54u$ ;  $dp = 67.75u$ , and diffusion conditions:  $As_4O = 1.12 \text{ atm.}$ , and chemically polished surface.  
 (B) at  $X = 9.7u$ ;  $d_0 = 39u$ ,  $dp = 42.5u$ , and diffusion conditions: chemically polished surface, and  $As_4O = .42 \text{ atm.}$   
 (C) at  $x = 74.25u$ ;  $d_0 = 74u$ ,  $dp = 105.25u$ , and diffusion conditions  $As_4O = .053 \text{ atm.}$ , and lapped surface.



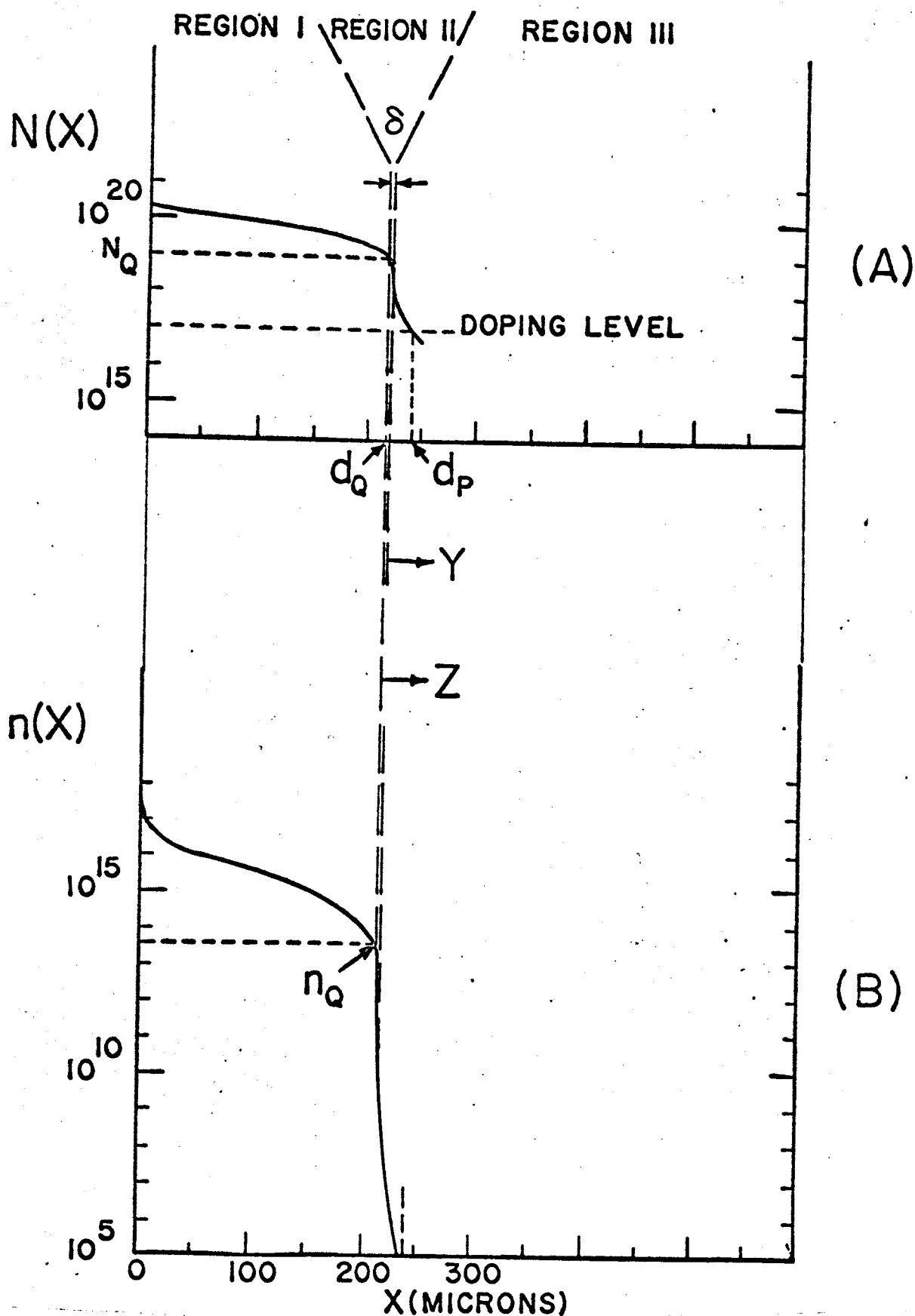


Figure 12. Three region moving band model: Region I for the high concentration, Region II for the sharp gradient where the leading edge of the dislocation band is, Region III for the low concentration of (A) the substitutional and (B) the interstitial species. Sample curves taken from equations (14) and (E-4).

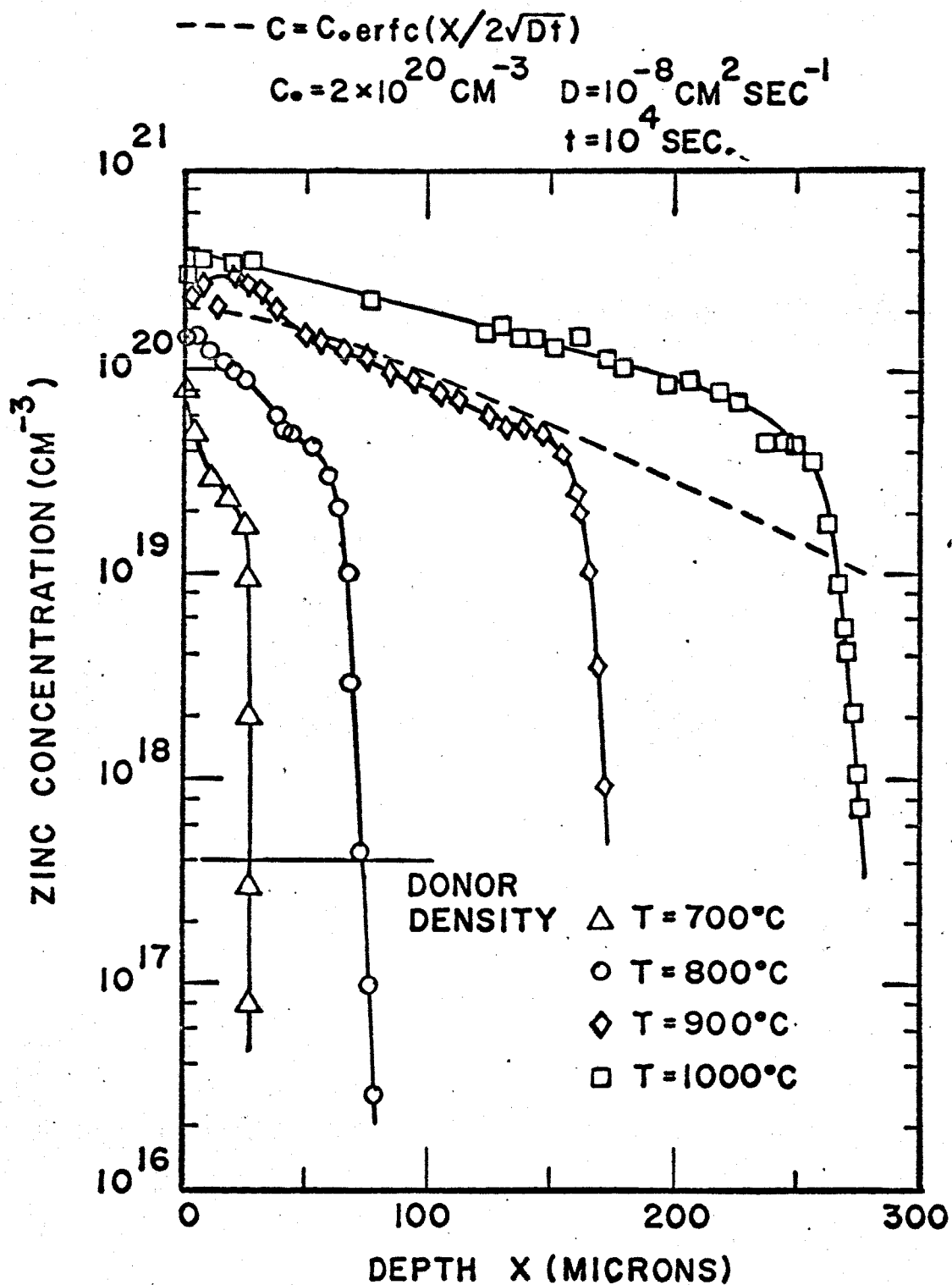


Figure 13. Diffusion profiles of zinc in gallium arsenide at 700°C, 800°C, 900°C, and 1000°C (by Chang and Pearson, October, 1963).

in each run. This assumption seems reasonable and the characteristic knee of the observed diffusion profile remains more or less constant even for temperature variations ranging from 800°C to 1000°C. At a given temperature, therefore, the assumption seems adequately justified. Fig. 12B shows the interstitial concentration profile which corresponds roughly to the zinc substitutional concentration profile of Fig. 12A.

#### ANALYSIS FOR REGION I.

The governing diffusion equation may be approximated by:

$$\frac{\partial n}{\partial t} = D \frac{\partial^2 n}{\partial x^2} - \frac{n - n_0}{\tau_1} \quad (1)$$

where  $n$  is the interstitial species concentration,  $D$  is the diffusion coefficient for interstitial species,  $\tau_1$  is the effective transition time constant for transition to substitutional positions in Region I,  $x$  and  $t$  are the distance and the time respectively,  $n_0$  is the equilibrium interstitial zinc concentration.

The transition time constant,  $\tau$ , which applies to all three regions, represents the "lifetime" of an atom in interstitial sites. As it jumps from one interstitial to another interstitial site, it finally jumps into an interstitial site which is the nearest-neighbor to a (gallium) vacancy. It is then assumed that it becomes substitutional.

It can be shown that, from probability considerations of jumps that an interstitial makes in GaAs to get into a nearest-neighbor site of a vacancy, the transition time can be expressed as

$$\tau = \frac{a^2 N_{Gs}}{8D} \frac{1}{N_v} \quad (2)$$

The transition time constant as expressed in equation (2) is a function of the vacancy concentration and can be evaluated using the average vacancy concentration that is available for the transition in Region I. At a given diffusion condition (temperature and excess arsenic) we assume that the vacancy equilibrium is maintained. Even though this is

probably not true, the actual vacancy density will probably be roughly proportional to its equilibrium value. The transition time constant, because of the assumed proportionality, contains the reaction rate constant (between the interstitials and the vacancies) and the probable frequency constant for the reaction to take place.

Equation (1) applies for  $0 \leq x \leq d_0$ . The first term on the right hand side describes the diffusion of interstitials into the volume element. The second term accounts for the net transition rate between the interstitials jumping into substitutional positions and the interstitials generated from substitutionals. The general solution of the diffusion equation (1) is expressed as

$$n - n_0 = [A_1 \exp(\alpha_1 x) + A_2 \exp(-\alpha_1 x)] \exp(M_1 t) \quad (3)$$

where  $A_1$ ,  $A_2$ , and  $M_1$  are arbitrary constants. We impose the following boundary conditions on equation (3): The experimental condition that the source at the surface is constant is,

$$n(0, t) - n_0 = n_s; t > 0 \quad (4)$$

where  $n_s$  is the constant excess interstitial concentration at the surface. The boundary condition at  $x = d_0$  is assumed as

$$n(d_0, t) - n_0 = 0 \quad (5)$$

As we will note this is only to be taken as an approximation for the solution in Region I. The excess interstitial flux, which resulted from the supersaturation of interstitials in Region I, supplies the "material" needed for the movement of the steep knee, which keeps the substitutional concentration at the boundary between Region I and II at  $N_Q$ . Thus we have

$$-D \frac{\partial n}{\partial x} \Big|_{x=d_0} = N_Q \frac{d(d_0)}{dt} \quad (6)$$

The boundary condition for the band motion is clearly not precise, but it is assumed that this is by far the major "function" of the diffusion process in Region I. Applying the boundary conditions, equations (4) and (7), to the general solution, equation (3), we obtain

$$n - n_0 = n_s \frac{\sinh \alpha_1 (d_0 - x)}{\sinh \alpha_1 d_0} \quad (7)$$

where  $\alpha_1^2 = [M_1 + (1/\tau_1)]/D$ , where  $M_1$  is a constant to be evaluated by further consideration. The particular solution, equation (7), is valid for the quasi-stationary conditions where  $d(d_Q)/dt$  is treated as though it were a constant or a small perturbation as far as Region I is concerned. Imposing the boundary condition for the band motion, equation (6), on equation (7) we obtain

$$\frac{Dt n_s}{d_Q^2 N_Q} = \frac{\cosh \alpha_1 d_Q - 1}{(\alpha_1 d_Q)^2} \quad (8)$$

which is a useful transcendental equation in determining  $\alpha_1$ .

The rate at which substitutionals are formed at a point  $x$ , is given by the second term (right hand side) in the diffusion equation (1). Thus, the substitutional concentration in Region I can be obtained from the relation

$$N(x) = \int_{t_1}^{t_d} \frac{n - n_0}{\tau_1} dt + N_Q \quad (9)$$

The substitutional concentration in Region I is assumed to be at  $N_Q$  at the start. Actually this is accomplished mathematically by having  $d_Q = 0$  at  $t = 0$ . The lower limit,  $t_1$ , of the integral is the time of arrival of  $d_Q$  at the selected  $x$ , and the upper limit  $t_d$  is the diffusion time.

For the case where the diffusion coefficient is independent of time and position, and where the diffusion profile can be represented by a complementary error function, the diffusion depth,  $d_Q$ , can be expressed as  $d_Q = \gamma t^{\frac{1}{2}}$  where  $\gamma$  is the boundary motion constant. The approximation expression for the concentration in Region I by a complementary-error-function is a reasonable one in view of the experimentally obtained diffusion profile having nearly the complementary-error-function curve in the corresponding region, and also in view of the time dependent measurement of  $d_Q$ , which indicated a relation,  $d_Q \cong \gamma t^{\frac{1}{2}}$ . Thus we assume that the band motion may be expressed

approximately by  $d_0 = \gamma t^{\frac{1}{2}}$ . Hence, from equation (9) we have an expression for the substitutional concentration in Region I as,

$$N(x) = \frac{n_s}{T_1} \left\{ (t_d - t_1) \cosh \alpha_1 x - \frac{2 \sinh \alpha_1 x}{\alpha_1 \gamma} + \left( t_d^{\frac{1}{2}} \ln \left| \sinh \alpha_1 \gamma t_d^{\frac{1}{2}} \right| - t_1^{\frac{1}{2}} \ln \left| \sinh \alpha_1 \gamma t_1^{\frac{1}{2}} \right| \right) \right\} + N_0 \quad (10)$$

For Region II the governing diffusion equation must account for the motion of the moving boundary between region I and II, which is assumed to move at an approximate rate of  $\gamma t^{\frac{1}{2}}$ . The motion of the moving boundary can best be accounted for by transforming the diffusion equation for the stationary coordinate system into the moving coordinate system,  $(z, t)$ , where  $z = x - \gamma t^{\frac{1}{2}}$ , and  $t' = t$ . Thus the result of the transformation can be written as

$$\frac{\partial n}{\partial t} = D \frac{\partial^2 n}{\partial z^2} + \frac{1}{2} \gamma t^{-\frac{1}{2}} \frac{\partial n}{\partial z} - \frac{n - n_2}{T_2} \quad (11)$$

The general solution for the diffusion equation (11) is

$$n(z, t') - n_2 = \left\{ B_1 \exp \alpha_2 (z - \gamma t^{\frac{1}{2}}) + B_2 \exp [-\alpha_2 (z - \gamma t^{\frac{1}{2}})] \right\} \exp (M_2 t) \quad (12)$$

where  $\alpha_2^2 = [M_2 + (1/T_1)]/D$ , and  $B_1$ ,  $B_2$ , and  $M_2$  are arbitrary constants. The boundary conditions are as follows: At  $x = d_0$  the continuity of the interstitial concentration can be written as

$$n(x = d_0^-, t) = n(z = 0^+, t) = n_0 \quad (13)$$

and the continuity of the gradient can be written as

$$\left. \frac{\partial n}{\partial x} \right|_{x = d_0^-} = \left. \frac{\partial n}{\partial z} \right|_{z = 0^+} \quad (14)$$

We impose the boundary conditions on the general solution (12), and obtain the following,

$$n(z, t) - n_2 = (n_0 - n_2) \cosh(\alpha_2 z) - \frac{\alpha_1 n_s \sinh \alpha_2 z}{\alpha_2 \sinh \alpha_1 d_0} \quad (15)$$

In defining the extent,  $\delta$ , of Region II the value of the interstitial concentration at the boundary between Regions II and III is taken as

$n_2$ , the fictitious equilibrium concentration in Region II. This fictitious equilibrium concentration is written as  $\beta n_0$  where  $\beta$  is an appropriate constant. Thus the following boundary condition for Region II can be written as

$$n(z = \delta^-, t) = n(y = 0^+, t) = \beta n_0 \quad (16)$$

Imposing the boundary condition on the particular solution, equation (15), yields the following:

$$\frac{\tanh \alpha_2 \delta}{\alpha_2 \delta} = \frac{n_0(1 - \beta) \sinh \alpha_1 d_0}{n_s \alpha_1 \delta} \quad (17)$$

The transcendental equation (17) can be used in determining the extent,  $\delta$ , of Region II.

The boundary between Regions II and III also moves into the crystal at an approximate rate of  $ut^{\frac{1}{2}}$  where  $u$  is the boundary motion constant. The motion of the boundary between Regions II and III should remain approximately equal to that of the boundary between Regions I and II so long as the extent,  $\delta$ , of Region II remains small and nearly a constant. Thus the motion of the boundary between Regions II and III expressed as  $ut^{\frac{1}{2}}$  can be a reasonable approximation. For Region III, therefore, it is convenient to convert the stationary system into a moving coordinate system,  $(y, t)$ . The result of the transformation can be written as

$$\frac{\partial n}{\partial t} = D \frac{\partial^2 n}{\partial y^2} + \frac{1}{2} ut^{-\frac{1}{2}} \frac{\partial n}{\partial y} - \frac{n}{\tau_3} \quad (18)$$

where  $y = x - ut^{\frac{1}{2}}$ , and  $u$  is the boundary motion constant. The general solution for the moving coordinate system is

$$n(y, t) = \left[ C_1 \exp[\alpha_3(y + ut^{\frac{1}{2}})] + C_2 \exp[-\alpha_3(y + ut^{\frac{1}{2}})] \right] \exp(M_3 t) \quad (19)$$

where  $\alpha_3^2 = [M_3 + (1/\tau_3)]/D$ , and  $C_1$ ,  $C_2$ , and  $M_3$  are arbitrary constants to be evaluated. The boundary conditions are as follows: The interstitials diffuse rapidly, but they find sites for transition to become substitutional atoms stopping far short of diffusion through the wafer. The boundary condition for the semi-infinite medium can be written as

$$n(y, t) \Big|_{y \rightarrow \infty} = 0 \quad (20)$$

The continuity of the gradient at the boundary of Region II and III can be written as

$$\frac{\partial n}{\partial y} \Big|_{y=0^+} = \frac{\partial n}{\partial z} \Big|_{z=\delta^-} \quad (21)$$

We impose these boundary condition equations (16), (20), and (21) on equation (19) and obtain,

$$n(y, t) = \beta n_0 \exp(-\alpha_3 y) \quad (22)$$

and an expression for  $\alpha_3$  is expressed as

$$\alpha_3 = \frac{1}{\beta} \left[ \frac{n_s \alpha_1}{n_0 \sinh \alpha_1 d_0} \cosh(\alpha_2 \delta) - (1 - \beta) \alpha_2 \sinh \alpha_2 \delta \right] \quad (23)$$

Equation (22) gives the interstitial distribution in the moving coordinate system  $(y, t)$ . Hence, we can convert it back to the stationary system using the relation,  $y = x - ut^{\frac{1}{2}}$  where  $u$  can be expressed in terms of the motion constant,  $\gamma$ , for the boundary between Regions I and II and the extent,  $\delta$ , of Region II as  $ut^{\frac{1}{2}} = \delta - \gamma t^{\frac{1}{2}}$  which can be seen in Figure 20. Thus we obtain,

$$n(x, t) = \beta n_0 \exp[-\alpha_3(x - \delta - \gamma t^{\frac{1}{2}})] \quad (24)$$

The rate at which substitutionals are formed at a point  $x$  in Region III is given by  $n(x, t) / \tau_3$ . Then the substitutional concentration can be obtained by integrating the rate over a period,  $t = t_d$  where  $t_d$  is the diffusion time. Hence,

$$N(x) = \frac{1}{\tau_3} \int_0^{t_d} n(x, t) dt \quad (25)$$

At the p-n junction the substitutional concentration is equal to the impurity doping level of the substrate, and hence  $N(x = d_p) = N_p$ , where  $d_p$  is the junction depth, and  $N_p$  is the impurity doping level of the substrate. Substituting equation (24),  $N_p$ , and integrating over  $t$ , we obtain an equation:



$$(d_p - d_Q) \alpha_3 = \ln(2 \beta n_Q) / (N_p \alpha_3 T_3 \gamma) + \alpha_3 \delta + \frac{1}{2} \ln(t_d) \quad (26)$$

From the equations 2, 8, 17, 23, and 26, we can calculate  $T_1$ ,  $T_2$ ,  $T_3$ , and  $\delta$  if such parameters as  $d_p$ ,  $d_Q$ ,  $N_p$ , and  $t_d$ , plus the diffusion coefficient,  $D$  and the diffusion profile are known. The absolute values of  $d_p$ ,  $d_Q$ ,  $N_p$ , and  $t_d$  are readily obtained from our diffusion data, but we lack information on  $D$  and the diffusion profile. Chang and Pearson obtained the information that we lack, from their is-concentration experiments. They reported the effective diffusion coefficient,  $\mathcal{D}$ , at 900°C for various zinc concentrations. We shall make use of their data in addition to ours to verify qualitatively the characteristics of  $T$  and  $\delta$ , under various diffusion conditions. The flux equation can be written with the concentration gradient and the diffusion coefficient of the interstitial species, and it can also be written with the concentration gradient of the substitutional species and the effective diffusion coefficient,  $\mathcal{D}$  as

$$F = -D \frac{dn}{dx} = -\mathcal{D} \frac{dN}{dx} \quad (27)$$

with the approximate relation,  $n = AN^y$  between the interstitial and the substitutional concentration obtained from Chang and Pearson, equation (27) yields a relation such as

$$\mathcal{D} = D y \frac{n}{N} \quad (28)$$

where  $A$  and  $y$  are constants. Hence the calculations for  $T$  and  $\delta$  are possible.

In order to account for the case of the excess arsenic being introduced during the run, the effective diffusion coefficient,  $\mathcal{D}_s$ , evaluated at the surface can be written as

$$\mathcal{D}_s ([As_4], T) = \mathcal{D}_s^0 ([As_4]_{dis}, T) \left[ \frac{[As_4]_{dis}}{[As_4]} \right]^{\frac{1}{4}} \quad (29)$$

where  $[As_4]_{dis}$  is the dissociation pressure<sup>(7)</sup> of the arsenic over the solid GaAs at  $T$ , and  $\mathcal{D}_s$  refers to the effective diffusion coefficient obtained without the excess arsenic.

In order to account for the surface damage such as the lapped surface of the sample, Region I is subdivided into two sections and the surface boundary conditions (at  $x = 0$ ) are moved for a distance  $L$ , which is the depth of the damaged layer. Jones and Hilton<sup>(8)</sup> reported from the infrared reflectivity measurements that the extent of the damage in GaAs is shown to be about equal to the diameter of the final grinding particles. Thus  $L$  can be determined.

The results of the calculated values are examined in view of the experimental observations, and are discussed in Section V.

## V. DISCUSSION

It has been observed that the etch pit band,  $Q$ , on the cleaved  $\{110\}$  surface, displays several grades of sharpness, and that the grades of sharpness is also displayed by the etch pit density profile as shown in Figures 3 and 4. Thus the grades of sharpness displayed by the etch pit band,  $Q$ , on the cleaved  $\{110\}$  surface can be used to represent the extent of the dislocation Band. An acute grade of the sharpness displayed by the etch pit band,  $Q$ , implies a small extent of the dislocation band, whereas a degradation of the sharpness implies a greater extent of the band. It is then clear that the extent of the dislocation band observed in Fig. 3 is smaller than that of Fig. 4. The extent of the dislocation band can be represented by the extent,  $\delta$ , of Region II as defined in the moving band model. The grade of the sharpness displayed by the etch pit band becomes degraded with the increasing extent,  $\delta$ , and for large  $\delta$  ( $\geq 0.2$  microns) the degradation becomes so pronounced that the etch pit band,  $Q$ , becomes almost indistinguishable from the background. Figure 14 shows the calculated  $\delta$  against the excess arsenic pressure.  $\delta$  decreases with the increasing excess arsenic, which is the trend in agreement with the observed extent of the dislocation band. i.e., the extent of the band with  $[As_4] = .42$  atm. in Fig. 15A is clearly shown smaller than that of the  $[As_4] = 0.015$  atm. shown in Fig. 15B. Another measure of the extent of the dislocation band can be shown by the relative variation of the transition time constant,  $\tau_2$ , in comparison to that of  $\tau_1$ , and  $\tau_3$ . The smaller  $\tau_2$ , the

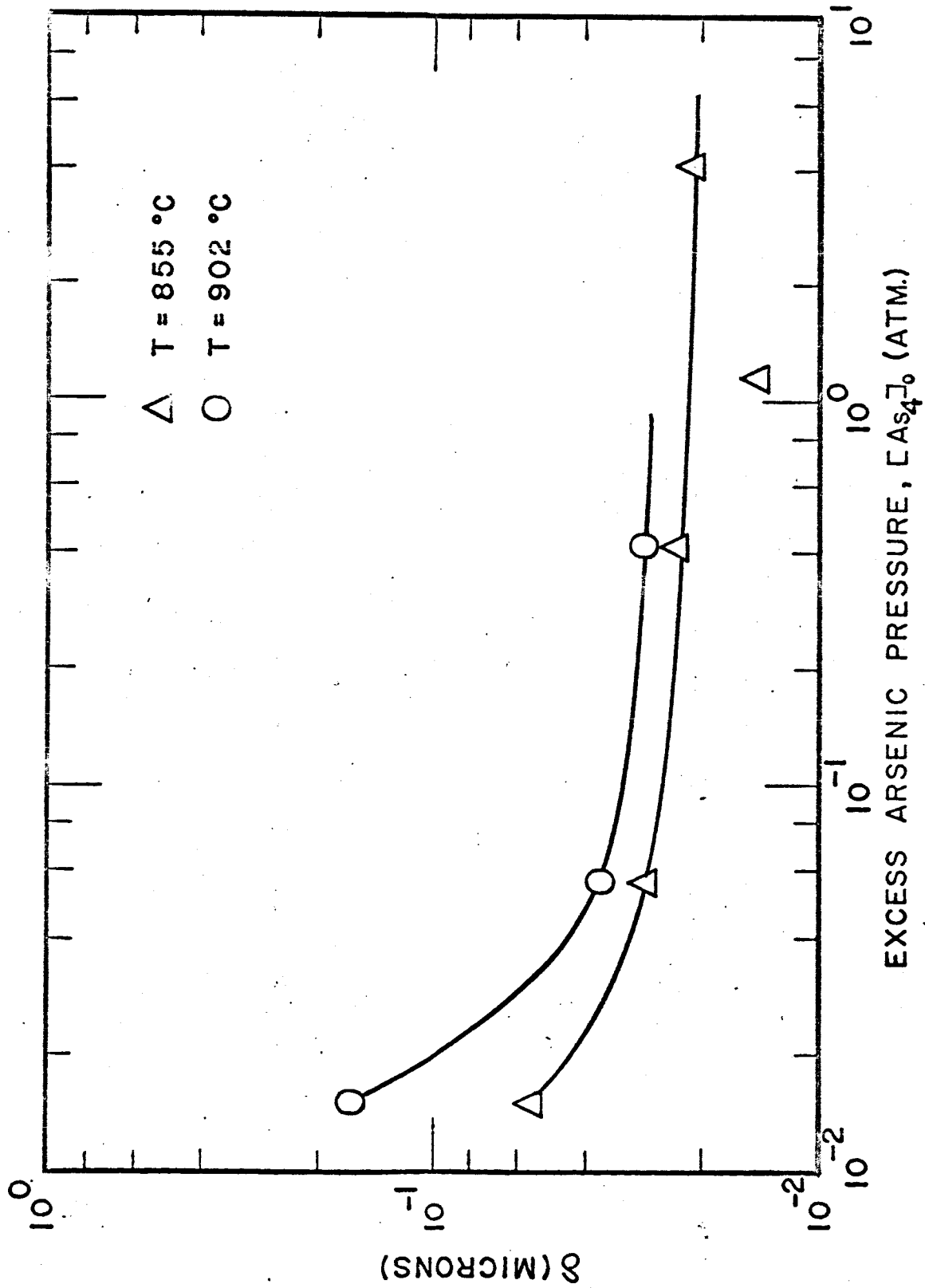
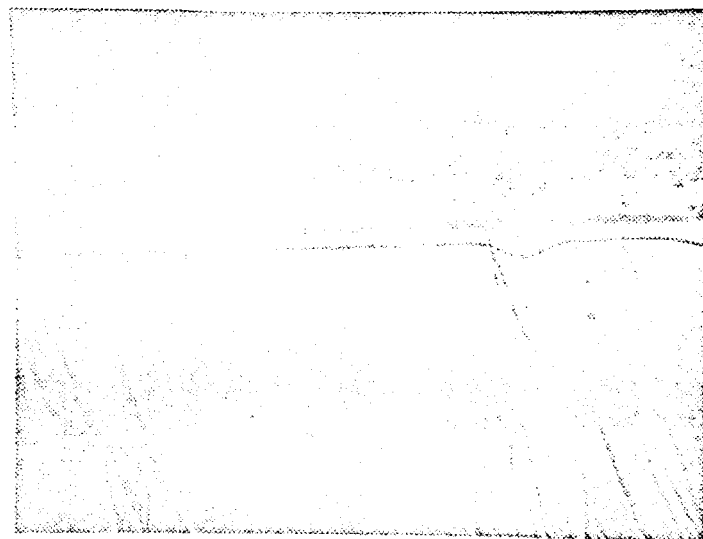
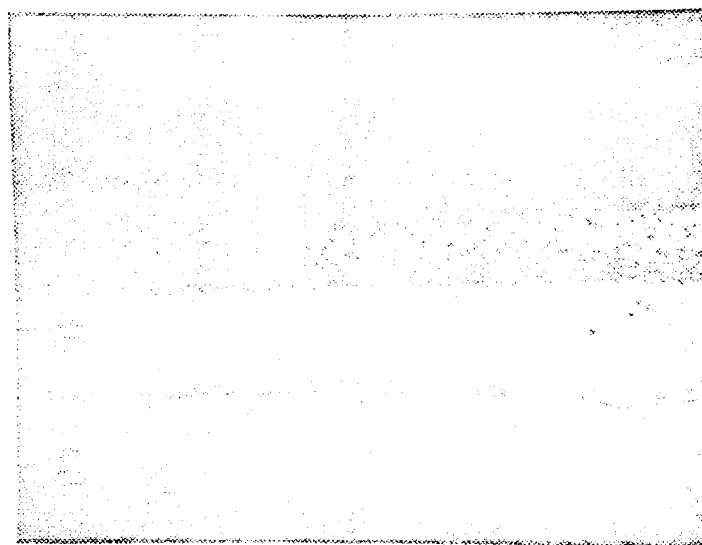


Figure 14. The calculated  $\delta$  against the excess arsenic pressure,  $As_4$ , at  $T = 855^\circ C$  and  $T = 902^\circ C$ .



L-75  
200x

(A)



L-73  
200x

(B)

Figure 15. Photomicrographs of the depth and the sharpness of Q, and P. Diffusion conditions:  
 (A)  $T = 902^{\circ}\text{C}$  and  $\text{As}_4\text{O} = .42 \text{ atm.}$   
 (B)  $T = 902^{\circ}\text{C}$  and  $\text{As}_4\text{O} = .015 \text{ atm.}$   
 Chemically polished surface and  $t_d = 3 \text{ hrs.}$

greater is the density of dislocations, and hence the smaller the extent,  $\delta$ , of Region II. Figure 16 shows the calculated  $T_1$ ,  $T_2$ , and  $T_3$  against the excess arsenic pressure. All the transition time constants increase with the decreasing excess arsenic, but  $T_2$  increases at a greater rate than  $T_1$ , or  $T_3$  at the low excess arsenic pressure ranges (e.g.  $< 0.1$  atm.). The rapid increase of  $T_2$  at the low excess arsenic, therefore, indicates the pronounced increase in the extent of the dislocation band, which is in good agreement with the experimental results, e.g. Fig. 15A and B.

Fig. 17 shows  $\delta$  versus the diffusion temperature.  $\delta$  increases with the increasing diffusion temperature, which implies that the extent of the dislocation band increases with the increasing temperature. This is in agreement with the experimentally observed extent of the dislocation band as shown in Figures 15B and 9B. The extent of the dislocation band at  $902^\circ\text{C}$  is distinctly greater than that of  $855^\circ\text{C}$ . The calculated  $T$  as shown in Fig. 18 also indicates the increase in the extent of the dislocation band in confirmation to the above calculated result of  $\delta$ .

The surface condition affects also the extent of the dislocation band. The results of the calculations made one for the polished surface and the other for the lapped surface, are  $\delta = .16$  microns and  $T_2 = 2 \cdot 10^{-5}$  seconds for the lapped surface, and  $\delta = 0.06$  microns and  $T_2 = 2 \cdot 10^{-6}$  seconds for the polished surface. The data used for the calculations was obtained with having the diffusion conditions fixed except for the surface condition. The calculated results indicate that the extent of the dislocation band is increased by the increasing roughness of the surface. Fig. 9B shows the experimental observation of the extent of the band for the polished surface, and Fig. 10B shows that of the lapped surface. These observations are in good agreement with the calculated results.

The planarity of the p-n junction is predominantly dependent on the distribution of the sites for the transition from interstitial to substitutional positions. Since the host crystal is not perfect, there will always be non-uniform distribution of sites inherent to each sample. Hence, the planarity of the junction will be affected accord-

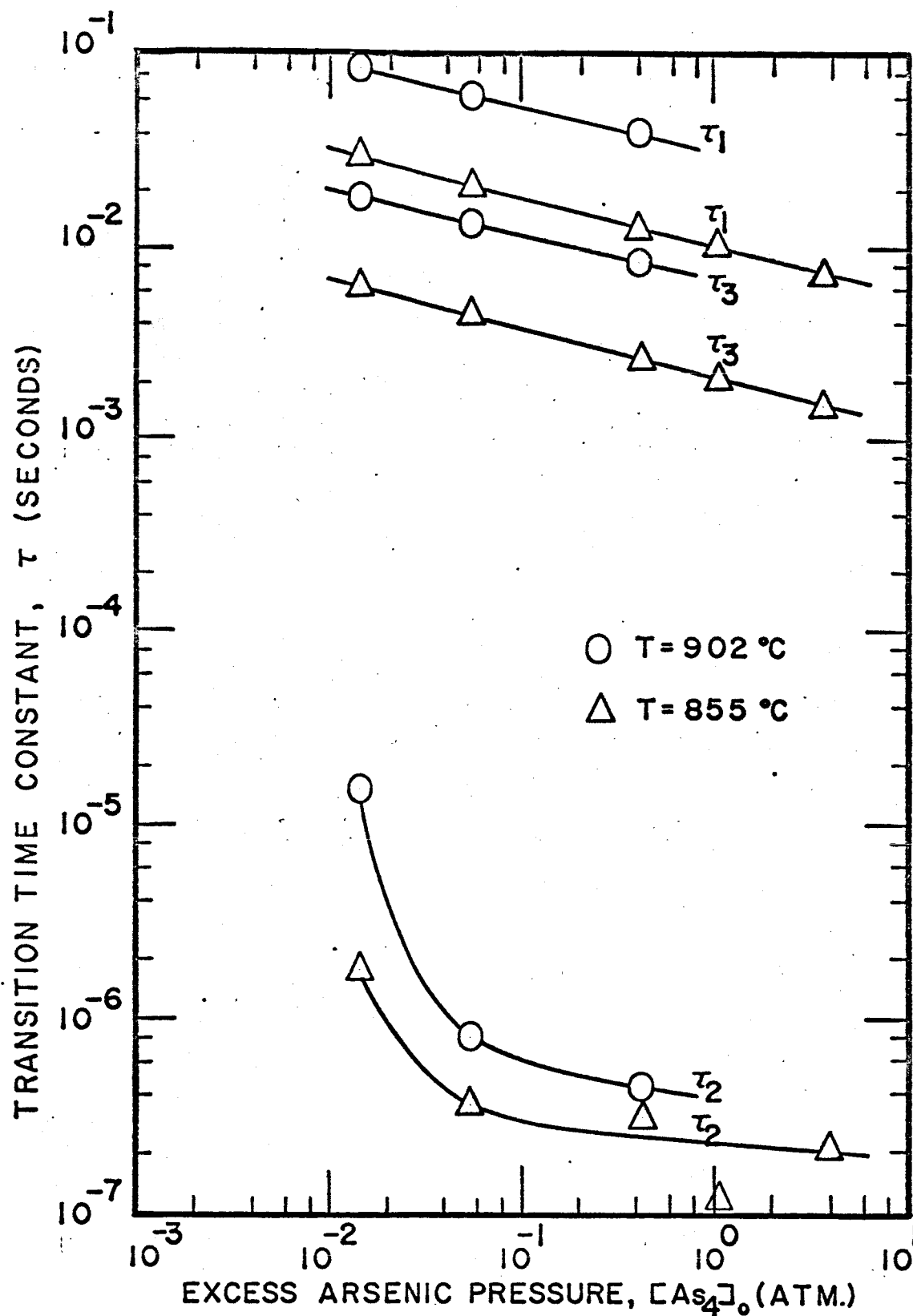


Figure 16. The calculated transition time constant,  $\tau$ , against the excess arsenic pressure,  $As_4$ , at  $T = 855^\circ C$  and  $T = 902^\circ C$ .

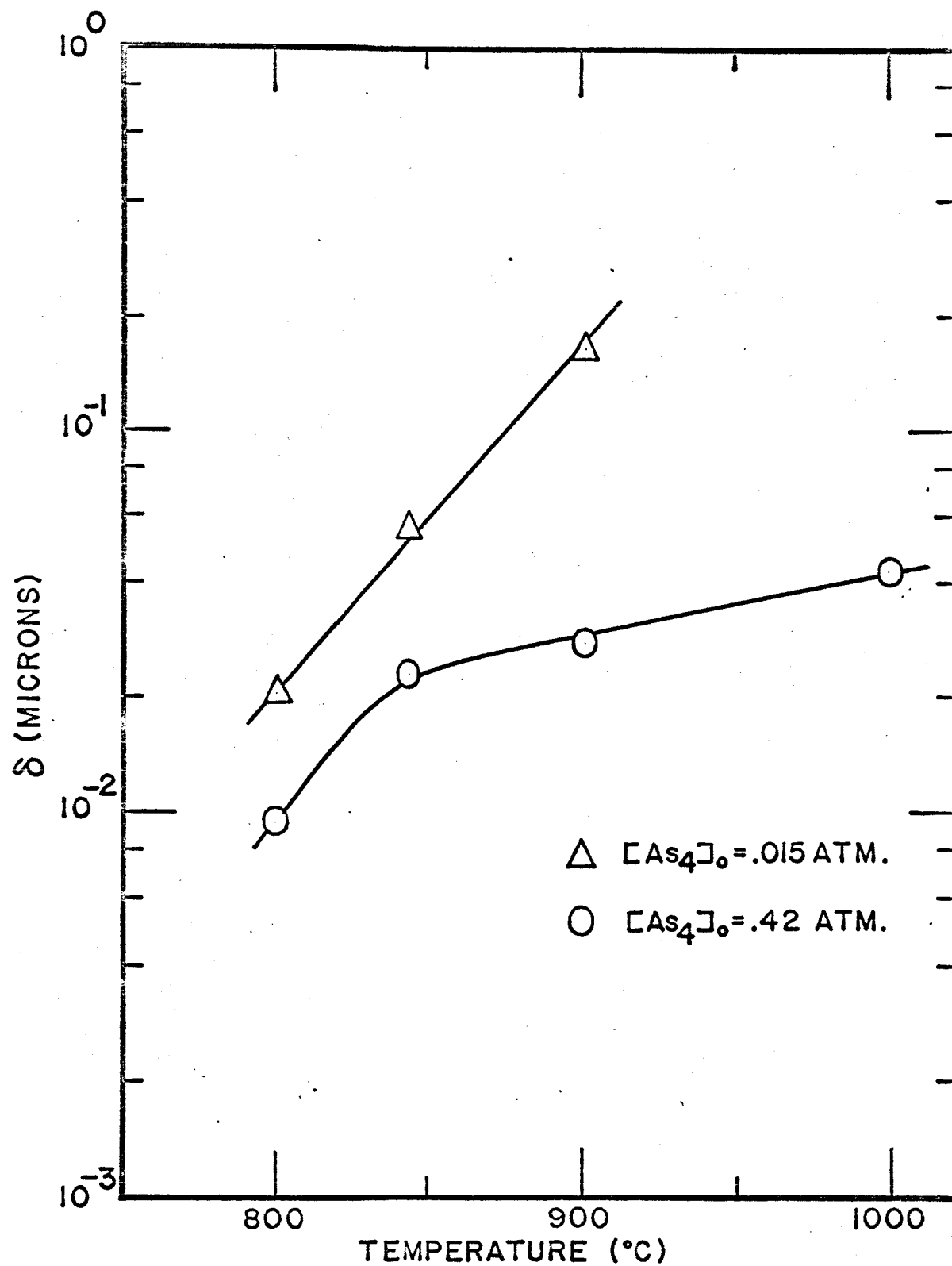


Figure 17. The calculated  $\delta$  against the diffusion temperature at  $\text{As}_4$   $_0 = .015$  atm. and  $\text{As}_4$   $_0 = .42$  atm.

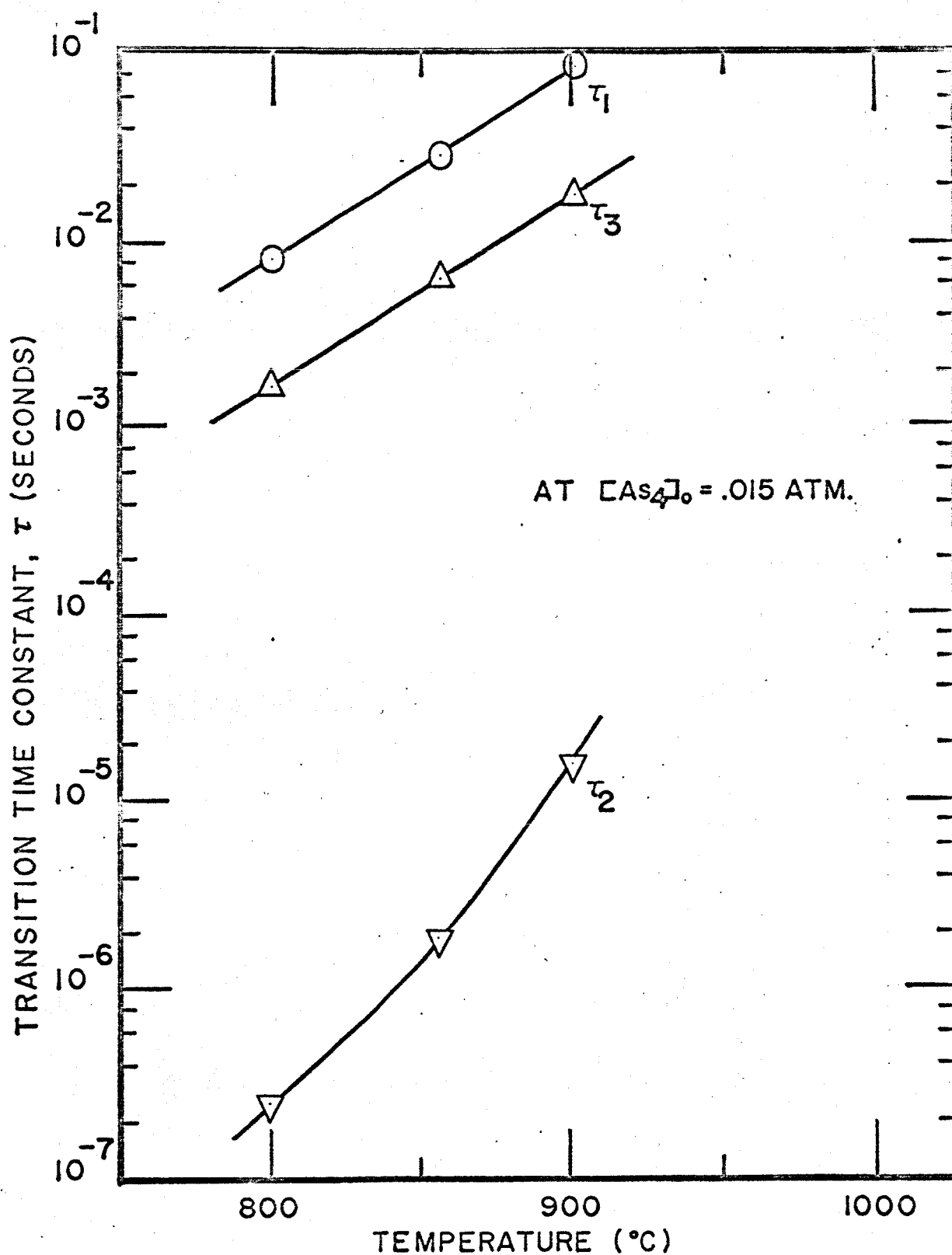


Figure 18. The calculated transition time constant,  $\tau$ , against the diffusion temperature at  $As_4$   $_0 = .015$  atm.



ingly. It was observed that the surface condition of the sample exhibits some influence on the uniformity of the etch pit distribution in the doped region as shown in Fig. 11A, B, and C. The sample in Fig. 11C had the lapped surface while the others shown in Fig. 11A, and B had the polished surfaces. The solute atoms when diffused into the host crystal, diffuse faster along the dislocations of the substrate and "condense" along the dislocation. Thus the resultant distribution is non-uniform, which attributes to the non-uniform distribution of the small etch pit density. Lapping the surface introduces randomly distributed dislocations near the surface, diminishing the effect of the non-uniformly distributed dislocations of the host crystal. Thus, the solute atoms have no longer preferred dislocation path through which they diffuse rapidly. Consequently the resultant distribution has improved uniformity, and a flatter p-n junction will be attained, i.e., the effect of the surface condition on improving the planarity as shown in Figs. 9B and 10B.

## VI. CONCLUSION

The moving dislocation band model introduced here have been shown qualitatively in good agreement with the experimental observations. It definitely accounts for the dislocation band observed in the diffused region when zinc has been the diffusant in gallium arsenide, and may also for the steep front of the characteristic knee in the diffusion profile although this front will be steep even without the dislocations. It also explains the experimentally observed results of the dependency of the zinc diffusion process on the diffusion conditions such as the diffusion temperature, the excess arsenic, and the surface condition. With the use of the non-uniform distribution of sites in Region III of the model for the interstitial-substitutional transitions, the lack of the planarity of the p-n junction is also explained. And finally, the moving dislocation band model presented here supports the concentration dependent diffusion mechanism involving the interstitial-substitutional species.

# REFERENCES

1. L. L. Chang and G. L. Pearson, "Diffusion Mechanism of Zinc in Gallium Arsenide and Gallium Phosphide Based on Isoconcentration Diffusion Experiments", J. Appl. Phys., V. 35, 1960-1965, (June, 1964), and "Diffusion, Solubility, and Distribution Coefficient of Zinc in Gallium Arsenide and Gallium Phosphide" RTD-TDR-63-4164, SEL-63-104, (Oct., 1963), RTD Technical Report.
2. R. L. Longini, "Rapid Zinc Diffusion in Gallium Arsenide", Solid-State Elect., V. 5, 127-130, (1962).
3. G. H. Schwuttke and H. Rupprecht, "X-ray Analysis of Diffusion-Induced Defects in Single Crystal Gallium Arsenide", Bull. Am. Phys. Soc., V. 10, 77(A), (1965).
4. H. A. Schell, "Atzversuche an Galliumarsenid", Z. Metallk., V. 48, 158-161, (1957).
5. M. S. Abrahams and L. Ekstrom, Properties of Elemental and Compound Semiconductors, Ed. H. C. Gatos, Interscience Publ., Inc., New York, N. Y., (1960).
6. T. E. Everhart, O. C. Wells, and R. K. Matta, "A Novel Method of Semiconductor Device Measurements", Proc. IEEE, V. 52, 1642-1647, (December 12, 1964).
7. J. Drowart and P. Goldfinger, "Etude Thermodynamique des Composes III-V et II-VI par Spectrometrie de Masse" J. De Chemie Physique V. 55, 721-732, (1958).
8. C. E. Jones and A. R. Hilton "The Depth of Mechanical Damage in Gallium Arsenide", J. Electrochem. Soc. 112, 9, 908-911, (September, 1965).

## GENERAL REFERENCE

- H. Rupprecht and C. Z. LeMay, "Diffusion of Zinc into Gallium Arsenide Under the Pressence of Excess Arsenic Vapor", J. Appl. Phys., V. 35, 1970-1973, (June, 1964).
- H. B. Kim, "Zinc Diffused P-N Junction for Gallium Arsenide Laser", Westinghouse Research Memo, 63-129-257-M1, 1-7, (Apr., 25, 1963).
- F. A. Cunnell and C. H. Gooch, "Diffusion of Zinc in Gallium Arsenide", J. Phys. Chem. Solids, V. 15, 127-133, (1960).
- H. C. Gatos and M. S. Lavine, "Characteristics of the III surfaces of the III-V intermetallic Compounds", J. Electrochem. Soc., 107, 433, (May, 1960).